Isotactic Polymers with Alternating Lactic Acid and Oxetane Subunits from the Endoentropic Polymerization of a 14-Membered Ring

Donghui Zhang, Jianyan Xu, Luis Alcazar-Roman, Loren Greenman, Christopher J. Cramer, Marc A. Hillmyer,* and William B. Tolman*

Department of Chemistry and Supercomputer Institute, University of Minnesota, 207 Pleasant Street SE, Minneapolis, Minnesota 55455-0431

Received March 3, 2004; Revised Manuscript Received April 17, 2004

ABSTRACT: A new isotactic, perfectly alternating polymer of (*S*)-lactic acid and oxetane was synthesized by the entropically driven ring-opening polymerization of a 14-membered cyclic diester (*S,S*-**3**) mediated by a zinc alkoxide catalyst. The polymer (*S,S*-PMOD) was characterized by NMR spectroscopy, size exclusion chromatography, and matrix-assisted laser desorption ionization mass spectrometry. Under polymerization conditions the equilibrium concentration (0.17 ± 0.05 M) of the monomer in toluene was essentially independent of temperature, and the average thermodynamic parameters for the ring-opening polymerization were found to be $\Delta H_p° = 0.2 \pm 0.7$ kJ mol^{-1} and $\Delta S_p° = +16 \pm 2$ J mol^{-1} K^{-1} (standard state [*S,S*-**3**] = 1.0 M). Theoretical calculations of the standard state enthalpy ($\Delta H_p°$) for ring-opening polymerization of various oxocyclics, including *S,S*-**3**, were well-correlated with experimental values. Kinetic studies showed that the polymerization of *S,S*-**3** was slower ($k_p = 0.82 \pm 0.04$ M^{-1} s^{-1} and $k_{dp} = 0.12 \pm 0.04$ s^{-1} at 25 °C) than that of lactide ($k_p = 2.2$ M^{-1} s^{-1}) using the same zinc alkoxide catalyst. Differential scanning calorimetry of *S,S*-PMOD showed a glass transition temperature of −30 °C for samples with molecular weights between 5 and 72 kg mol^{-1}. In support of the potential utility of *S,S*-PMOD as a PLA plasticizer, the complete miscibility of the polymeric components was demonstrated by the observation of single T_g values for a series of blends of *S,S*-PMOD and atactic PLA.

Introduction

Polylactide (PLA) is derived from a biorenewable resource and is a potential replacement for nondegradable petrochemical-based polymeric materials.[1] However, despite its high tensile modulus and tensile strength, PLA is inherently brittle. Different approaches have been taken to improve the ductility of PLA, including the preparation of copolymers or addition of plasticizers to form polymer blends, the latter being a common commercial tactic.[2−4] Addition of monomeric plasticizers can typically change the properties of bulk polymeric materials in a dramatic fashion,[5] but migration out of the bulk polymer over time makes small-molecule plasticizers less desirable, especially in food packaging or health-related applications. Thus, the development of macromolecular plasticizers for PLA is an important research objective.

Examples of polymeric or oligomeric systems that have been investigated for PLA plasticization include poly(3-hydroxybutyrate),[6] poly(ϵ-caprolactone),[7−9] thermoplastic starch,[10] oligomeric PLA,[11] poly(ethylene oxide) (PEO),[8,10,12−15] poly(vinyl acetate),[16] poly(butylene succinate),[17,18] poly(hexamethylene succinate),[19] oligomeric tributyl citrate,[20] and poly(3-methyl-1,4-dioxan-2-one) (PMDO, Scheme 1).[21] In most cases, the plasticizers are effective in lowering the glass transition temperature (T_g) of PLA and remain miscible up to a certain solubility limit, above which phase separation occurs. For example, PEO is miscible with PLA at high molecular weight ($M_w \approx 4000$ kg mol^{-1}) and at low loading levels (<50%)[12] and can improve the elongation at break and impact resistance of PLA.[22] However, one study on low molecular weight PEO ($M_w \approx 20$ kg mol^{-1}) in PLA blends showed that high PEO loadings (>50%) led to some separation of an amorphous phase that was induced by crystallization of the PEO component. This resulted in an overall increase in modulus and a corresponding decrease in elongation at break of the blends.[13]

Scheme 1

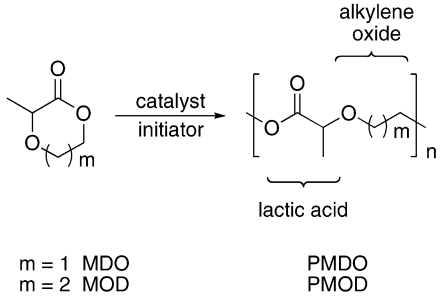

We postulate that perfectly alternating copolymers of lactic acid and alkylene oxides (Scheme 1) will serve as optimal macromolecular plasticizers for PLA due to a combination of miscibility and T_g control. We reason that miscibility will be enhanced due to the congruence of the lactic acid segment in the plasticizer with the PLA repeat unit and that the alkylene oxide segment in the plasticizer will enhance the flexibility of the polymer backbone and depress the T_g of the polymer and its PLA blend. In support of these notions, we prepared poly(3-methyl-1,4-dioxane-2-one) (PMDO), an alternating copolymer of lactic acid and ethylene oxide, and found that PMDO is miscible with atactic PLA in all proportions, has a T_g (≈−20 °C) much lower than that of atactic PLA (≈60 °C), and upon blending with PLA induces a lowering of its T_g.[21] With these results in hand, we have focused our efforts on even more efficient lowering of

* To whom correspondence should be addressed. Fax: (612) 624-7029. E-mail: (M.A.H.) hillmyer@chem.umn.edu, (W.B.T.) tolman@chem.umn.edu.

10.1021/ma049571s CCC: $27.50
Published on Web 06/10/2004

Scheme 2

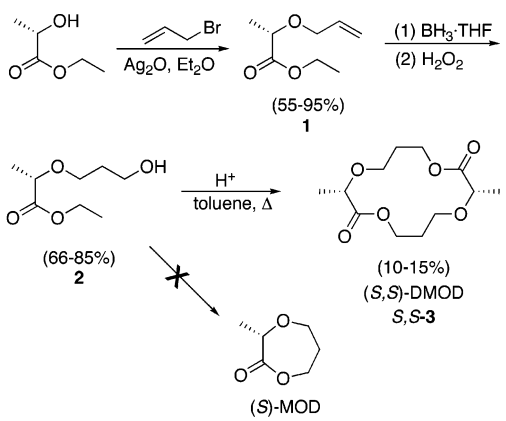

the T_g of PLA, which we envisioned might be achievable if the ethylene oxide segment of PMDO is replaced by another more flexible segment, such as oxetane. Indeed, the T_g of polyoxetane (≈−80 °C) is lower than that of PEO (−60 °C).[23]

The previous use of MDO to successfully prepare PMDO via a ring-opening polymerization led us to target MOD (Scheme 1) as a precursor to PMOD. Herein we report the results of our synthetic efforts, which led not to MOD but to its dimer, a 14-membered cyclic diester. Nonetheless, and despite initial concerns that a lack of strain in the 14-membered ring would be problematic, polymerization of this new monomer was successfully accomplished, yielding isotactic PMOD comprising perfectly alternating (*S*)-lactic acid and oxetane subunits. The thermodynamics of the polymerization reaction were investigated both experimentally and by theory, which rationalized the unusual finding that the polymerization is driven by changes in entropy, rather than enthalpy. In addition, the potential of isotactic PMOD as a plasticizer for atactic PLA was evaluated by differential scanning calorimetry (DSC).

Results and Discussion

Monomer Synthesis. In analogy with the previous synthesis of MDO,[21] we envisioned that MOD could be prepared by acid-promoted ring closure of **2**, which in turn could be derived from the biorenewable resource ethyl (*S*)-lactate (Scheme 2). Thus, ethyl (*S*)-lactate was coupled with allyl bromide in the presence of Ag_2O to yield **1**,[24] which was then oxidized to form **2**. No evidence for the formation of MOD was obtained upon treatment of **2** with *p*-toluensulfonic acid in refluxing toluene, however. Instead, (*S,S*)-DMOD (*S,S*-**3**) was obtained as a white crystalline solid in a 15% yield after column chromatography. Conclusive support for the formulation of *S,S*-**3** was obtained through ^{1}H and ^{13}C{^{1}H} NMR spectroscopy (Figure S1), FTIR spectroscopy, high-resolution mass spectrometry, optical rotation ($[\alpha]^{25}_D$ = −198.9°), and X-ray crystallography (Figure 1). Enantiomeric purity was confirmed by the X-ray structure, although the S configurations of the stereogenic centers were assumed on the basis of the stereochemistry of the ethyl (*S*)-lactate used as starting material in the synthesis. For comparative purposes, we also used the racemic precursor ethyl (*S*/*R*)-lactate, which led to a mixture of DMOD (**3**) stereoisomers identified as a 1:1 mixture of racemic (*S,S*/*R,R*) and meso (*S,R*) forms by NMR spectroscopy (and a lack of optical rotation). In addition, by taking advantage of solubility differences, we were able to obtain a sample of **3** enriched with 90% of the meso (*S,R*) form (^{1}H NMR spectrum in Figure S2).

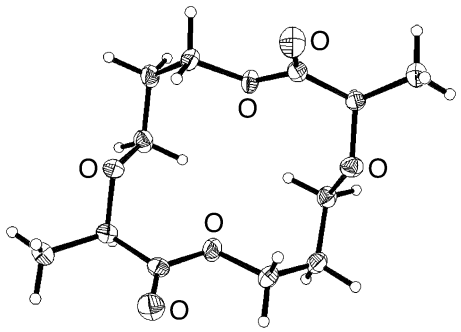

Figure 1. Representation of the X-ray crystal structure of *S,S*-**3**, as 50% thermal ellipsoids.

Scheme 3

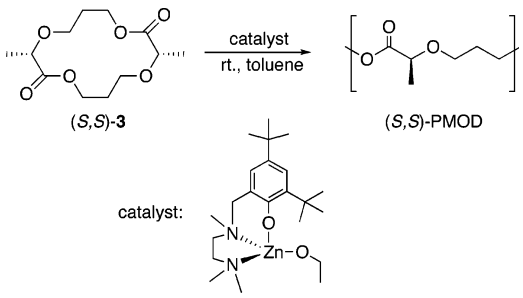

Table 1. Data for the Room Temperature Ring-Opening Polymerization of *S,S*-3[a]

$[3]_0/[Zn]_0$	convn (%)	M_n theor	M_n SEC	PDI	yield (%)
16[b]	88	4.2	4.9	1.7	60
50	90	12	13	1.9	73
100	90	23	26	1.7	77
200[c]	80	42	43	1.6	70
400[c]	80	83	72	1.6	75

[a] All molecular weights are in the unit of kg mol^{-1}; $[3]_0$ is the initial concentration of *S,S*-**3**; the theoretical M_n is based on the conversion from ^{1}H NMR spectra; reactions were quenched after 40 min. Conditions: room temperature, toluene, $[3]_0$ = 1.54 M except where noted. [b] $[3]_0$ = 1.38 M. [c] $[3]_0$ = 1.0 M.

Polymer Synthesis. Despite its large ring size that implicates little, if any, enthalpic ring strain that is typically required for ring-opening polymerizations, rapid formation of PMOD from **3** was effected by using a previously reported[25] zinc catalyst (Scheme 3, Table 1). For example, the reaction of *S,S*-**3** in toluene (120 mg, 0.46 mmol, 1.54 M) with the zinc catalyst (4.6 μmol, $[3]_0/[Zn]_0$ = 100) resulted in a 90% conversion to isotactic PMOD in less than 5 min.

The product of the polymerization of *S,S*-**3** was characterized by ^{1}H and ^{13}C{^{1}H} NMR spectroscopy (including two-dimensional ^{1}H/^{13}C data), matrix-assisted laser desorption ionization (MALDI) mass spectrometry, and size exclusion chromatography (SEC) data. The MALDI mass spectrum (Figure 2) of a low molecular weight sample (M_n = 4.3 kg mol^{-1}, PDI = 1.7 from SEC) exhibits peaks with masses corresponding to the sum of integral numbers of repeating unit (130.07), ethanol (46.07), and sodium ion (22.99) from the matrix. These data confirm the incorporation of an ethoxy end group inherited from the zinc catalyst. The average molecular weight (M_n = 3.1 kg mol^{-1}, PDI = 1.2) calculated from the MALDI-MS spectrum is in reasonable agreement with the molecular weight de-

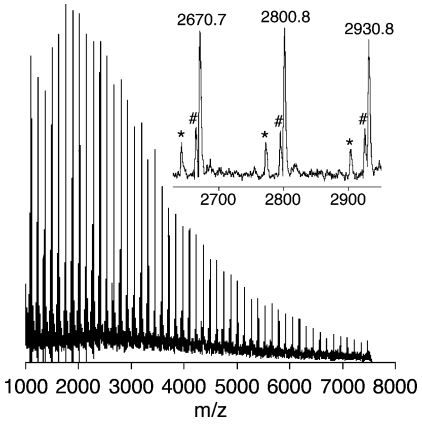

Figure 2. The MALDI-MS spectrum of low molecular weight *S,S*-PMOD (M_n = 4.3 kg·mol^{-1}, PDI = 1.7). See the text for assignments.

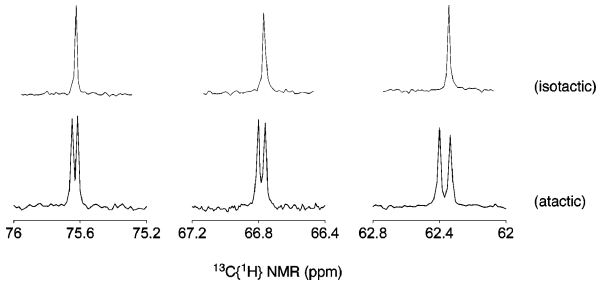

Figure 3. Regions of the ^{13}C{^{1}H} NMR spectra of isotactic *S,S*-PMOD and atactic PMOD showing resonances due to the methine and two methylene carbons.

termined by SEC (using polystyrene standards). We attribute the mass peaks labeled with * as cyclic esters formed from depolymerization "back-biting" of the PMOD (see below). Another minor set of mass peaks labeled with # was also observed in the MALDI spectrum, the origin of which is still under study.

NMR spectroscopy was used to assess the tacticity of the polymer derived from *S,S*-**3**, which was compared to the PMOD resulting from ring-opening polymerization of the 1:1 mixture of racemic and meso forms of **3** (Figures 3 and S3). In the ^{13}C{^{1}H} NMR spectra, the latter sample (presumably atactic PMOD) exhibits three sets of two equally intense resonances due to the methine carbon and two methylene carbons, whereas the PMOD from *S,S*-**3** shows only three peaks. To assign these spectra, we consider triad and dyad level analyses (Figure 4). Focusing on the methine carbon (labeled with an asterisk), four possible triads for atactic PMOD would result in four resonances in the ^{13}C{^{1}H} NMR spectrum. However, only two resonances are observed for the methine carbon, which we suggest is due to insensitivity of the NMR peak shifts to triad-level interactions. In other words, the presence of two resonances in the presumed atactic PMOD suggests that the methine carbon can only sense the difference in an adjacent chiral configuration in one direction of the polymer chain and not the other.[26] Therefore, we propose that the two sets of resonances in the ^{13}C{^{1}H} NMR spectrum of atactic PMOD derived from the 1:1 mixture of *S,S*/*R,R*-**3** and *S,R*-**3** arise from the two possible dyads shown in Figure 4 (right). The presence of only one set of peaks for the polymer derived from *S,S*-**3** thus are consistent with isotactic PMOD, which we propose is *S,S*-PMOD (the *i* dyad) under the reasonable assumption[25] that no epimerization *S,S*-**3** occurs during the polymerization reaction.

Polymer molecular weight control was assessed by removal of reaction aliquots and analysis of conversion by ^{1}H NMR spectroscopy and of polymer molecular weight and polydispersity by SEC. A linear increase of molecular weight with conversion was observed (Figure 5, left), consistent with the controlled nature of the polymerization, although polydispersities are somewhat broad (1.5−1.7). The results for the polymerization reactions with different initial monomer-to-catalyst ratios are summarized in Table 1. The number-average molecular weights (M_n) of the resulting polymers are consistent with the M_n values calculated for the initial monomer-to-catalyst ratios. As shown in Figure 5 (right), the M_n of the forming polymers increases with time, but after maximum conversion, the M_n starts to drop slowly over time. We suggest that the reduction of molecular weight is due to the irreversible formation of macrocyclic oligomers through an intramolecular transesterification mechanism that competes with the propagation of polymer chains. Such a "back-biting" mechanism to generate macrocyclic oligomers is documented for metal-complex-mediated ring−opening polymerizations of cyclic esters[27,28] and ester amides.[29] The proposed formation of cyclic oligomers is also supported by the MALDI-MS data (peaks with asterisks in Figure 2 and Figure S4), which display envelopes of mass peaks corresponding to the sum of an integral number of repeating units (130.07) and sodium ions (22.99, major) or potassium ions (39.10, minor) from the matrix and no ethoxy end groups.

Polymerization Kinetics and Thermodynamics. Polymerization rate data were acquired in order to compare the efficacy of the zinc catalyst for the polymerizations of **3** and LA. Thus, the ring-opening polym-

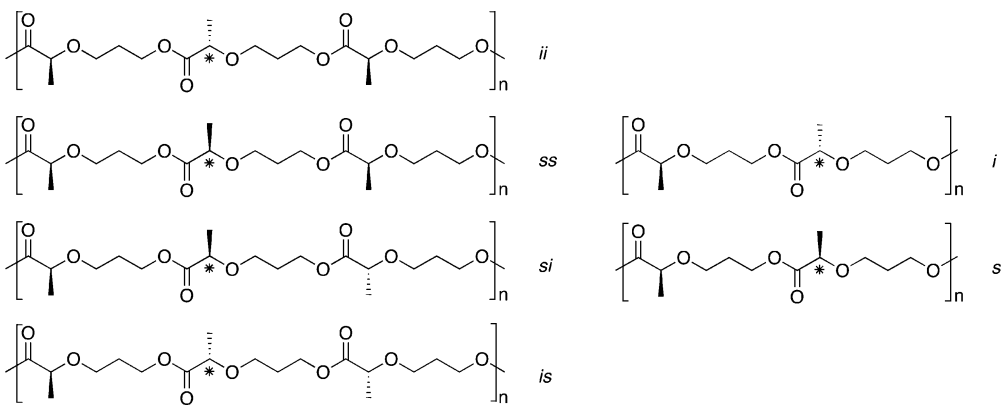

Figure 4. The stereochemistry of PMOD at the triad (left) and dyad (right) levels (*i* = isotactic pair, *s* = syndiotactic pair).

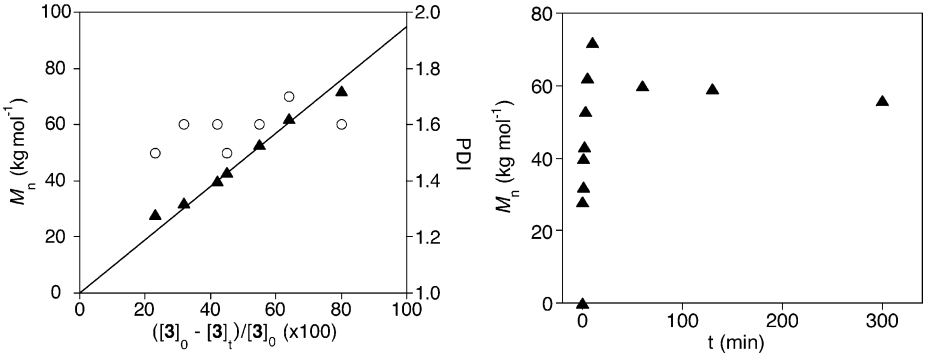

Figure 5. (left) Dependence of molecular weight (M_n, ▲) and polydispersity (PDI, ○) on conversion for the polymerization of *S,S*-**3**. (right) Dependence of molecular weight (M_n) on the reaction time. Conditions: toluene, room temperature, $[\mathbf{3}]_0 = 1.0$ M, $[\mathbf{3}]_0$:$[Zn]_0 = 400$.

erization of *S,S*-**3** in CH_2Cl_2 under the conditions $[\mathbf{3}]_0 = 0.5$ M, $[\mathbf{3}]_0/[Zn]_0 = 400$, at 25 °C was monitored in situ by FTIR spectroscopy (ReactIR). A typical decay of the peaks arising from *S,S*-**3** is shown in Figure S5, with an exponential first-order fit of the decay curve that yields the observed rate constant k_{obs}. Under the assumption of a first-order dependence on [Zn], this rate constant may be expressed as $k_{obs} = k_p[Zn]$, with the propagation rate constant $k_p = 0.82 \pm 0.04$ M^{-1} s^{-1} (average of three independent runs). For comparison, the rate constant for the polymerization step (k_p) of (D,L)-lactide measured previously under the same conditions is 2.2 M^{-1} s^{-1}.[25] In addition, the equilibrium constant for the polymerization of *S,S*-**3** may be defined as $K_{eq} = k_p/k_{dp} = 1/[\mathbf{3}]_{eq}$, where k_{dp} is the depolymerization rate constant. The conversion at equilibrium was determined from a ^{1}H NMR spectrum of a reaction aliquot and the equilibrium concentration of monomer was calculated to be $[\mathbf{3}]_{eq} = 0.15 \pm 0.01$ M. Using this value, the measured value for k_p, and the expression for K_{eq} (above), we calculate $k_{dp} = 0.12 \pm 0.04$ s^{-1} at 25 °C.

The thermodynamic parameters for the reversible polymerization of *S,S*-**3** were obtained by measuring $[\mathbf{3}]_{eq}$ at different temperatures and applying eq 1,[30]

$$\ln\left(\frac{[\mathbf{3}]_{eq}}{[\mathbf{3}]_{ss}}\right) = \frac{\Delta H_p^\circ}{RT} - \frac{\Delta S_p^\circ}{R} \qquad (1)$$

where ΔH_p° is the standard state enthalpy of polymerization, ΔS_p° is the standard state entropy of polymerization, and $[\mathbf{3}]_{ss}$ is the standard state solution concentration of *S,S*-**3** = 1.0 M. The equilibrium monomer concentrations were measured by ^{1}H NMR spectroscopy using three different $[\mathbf{3}]_0$ between 0 °C and 100 °C, with 1−5 mol % catalyst. To ensure that equilibration had been reached and that polymerization had not terminated due to catalyst deactivation, at the end of each experiment additional *S,S*-**3** was added; in each case, polymerization re-ensued. The temperature dependences of $[\mathbf{3}]_{eq}$ for each value of $[\mathbf{3}]_0$ are shown in Figure 6. Linear fits of each set of data gave values of ΔH_p° and ΔS_p° using eq 1 for each $[\mathbf{3}]_0$. As shown in Figure 6, the $[\mathbf{3}]_{eq}$ values at 25 °C are essentially independent of $[\mathbf{3}]_0$. Therefore, we averaged the three values of ΔH_p° and ΔS_p° obtained from the three linear fits. This resulted in an average $\Delta H_p^\circ = 0.2 \pm 0.7$ kJ mol^{-1} and an average $\Delta S_p^\circ = +16 \pm 2$ J mol^{-1} K^{-1}. These values indicate that *S,S*-**3** has very little, if any, ring strain and that its ring-opening polymerization is entropically driven. At room temperature the equilibrium monomer concentration for **3** is quite small, and therefore, a high concentration of

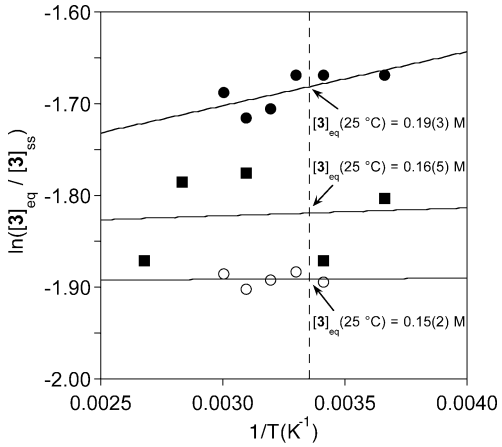

Figure 6. The temperature dependence of the equilibrium monomer concentration of **3** at various $[\mathbf{3}]_0$. $[\mathbf{3}]_0 = 1.54$ M and $[Zn]_0 = 15.4$ mM (filled squares); $[\mathbf{3}]_0 = 0.60$ M and $[Zn]_0 = 15.8$ mM (filled circles); $[\mathbf{3}]_0 = 0.26$ M and $[Zn]_0 = 13.7$ mM (open circles). The lines are linear fits of the data (eq 1). The three calculated values for $[\mathbf{3}]_{eq}$ are given at 25 °C (marked by the vertical dashed line).

Scheme 4

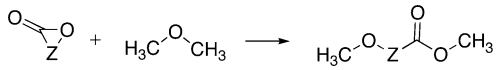

monomer typically needed to favor polymer in entropically driven (or weakly enthalpically driven) polymerizations is not necessary in the case of **3**. Normally, cyclic esters with smaller ring sizes undergo ring-opening polymerization driven by the release of ring strain ($\Delta H_p^\circ < 0$) and a concomitant loss of entropy ($\Delta S_p^\circ < 0$),[21,27,37] although entropically driven reactions have been reported for macrocycles with ring sizes > 12.[31−34] The most relevant report describes the ring-opening polymerization of 15-pentadecanolactone in the melt, for which $\Delta H_p^\circ = 3.0$ kJ mol^{-1} and $\Delta S_p^\circ = 23$ J mol^{-1} K^{-1}.[35] Such results may be rationalized qualitatively by arguing that the large macrocycles have low ring strain and limited conformational freedom, the latter of which increases significantly upon ring-opening to form linear polymers.

To assess the notion that *S,S*-**3** lacks significant ring strain, as implied by the measured ΔH_p° value, we sought to develop an efficient computational approach for estimating the solution-state enthalpy of polymerization. We considered the reaction in Scheme 4 as an analogue for ring-opening polymerization, where Z represents an arbitrary linking functionality (e.g., Z = $-CH_2CH_2CH_2-$ corresponds to γ-butyrolactone). The

Table 2. Experimental and Theoretical Ring-Strain Energy Measures (kJ mol^{-1})

molecule	ΔE^a	$\Delta H_p°$ [b]	ref
L-lactide	−86.2	−22.9	37
1,4-dioxan-2-one	−60.7	−14.1	38
ϵ-caprolactone	−58.4	−14.0	39
3-methyl-1,4-dioxan-2-one	−58.6	−12.1	21
D-valerolactone	−64.7	−8.4	39
S,S-**3**	−26.9	0.2	this work

[a] Calculated in this work for the reaction in Scheme 4. [b] Measured solution state enthalpies of ring-opening polymerization.

reaction in Scheme 4 is an isodesmic equation, which is to say that the two sides of the chemical equation are balanced and that each contains the same number and "type" of all chemical bonds. This feature of isodesmic equations permits the use of relatively inexpensive levels of electronic structure theory for the evaluation of the energy of reaction, insofar as errors in approximate levels of theory for particular kinds of bonds/functionality tend to cancel in computation of the energy *change*. As such, the reaction in Scheme 4 may be considered to be a computational model for ring strain[36] (offset by some arbitrary amount associated with the higher order changes in bond types that occur).

We computed ΔE electronic energy values for the reaction in Scheme 4 at the HF/MIDI! level (see Computational Methods) and compared these values to the previously reported experimental solution state enthalpies of polymerization ($\Delta H_p°$) for five compounds, namely, L-lactide,[37] 1,4-dioxan-2-one,[38] ϵ-caprolactone,[39] 3-methyl-1,4-dioxan-2-one,[21] and δ-valerolactone[39] (Table 2). A linear correlation between the theoretical and experimental quantities was determined as

$$\Delta H_p° = 0.37\Delta E + 9.72 \text{ kJ mol}^{-1} \qquad (2)$$

with a Pearson correlation coefficient R of 0.804 (Figure S6). Other approaches were assessed for computing ΔE, including adding ethyl acetate or toluene solvation free energies, computing electronic energies at the density functional level of theory, and/or rigorously accounting for conformational diversity by carrying out a Boltzmann average over all HF/MIDI! minima within 12 kJ mol^{-1} of the global minimum. However, none of these computationally more costly protocols led to a correlation improved over that of eq 2.

At the HF/MIDI! level, the ΔE value computed for *S,S*-**3** is −26.9 kJ mol^{-1}. Using this value in eq 2 results in a predicted $\Delta H_p°$ value of −0.1 kJ mol^{-1}—a prediction that agrees with our experimental measurement to within 0.3 kJ mol^{-1}. While such nearly perfect quantitative agreement is clearly fortuitous, the important point to note is that the computational protocol associated with Scheme 4 is highly efficient and capable of providing rapid estimates of $\Delta H_p°$ for relevant substrates.

Thermal Properties of *S,S*-PMOD and Blends with PLA. Using differential scanning calorimetry (DSC), we measured the T_gs of several samples of *S,S*-PMOD with molecular weights between 5 and 72 kg mol^{-1}. We found that the T_g of *S,S*-PMOD was ca. −30 °C for all samples. This value is significantly less than that of atactic PLA ($T_g \approx 60$ °C) and slightly lower than that of PMDO ($T_g \approx -20$ °C). Atactic PMOD displayed a similar glass transition temperature ($T_g = -32$ °C, $M_n = 21$ kg mol^{-1}, PDI = 1.9). There was no indication by DSC of melting or crystallization of either isotactic or atactic PMOD between −100 and 180 °C.

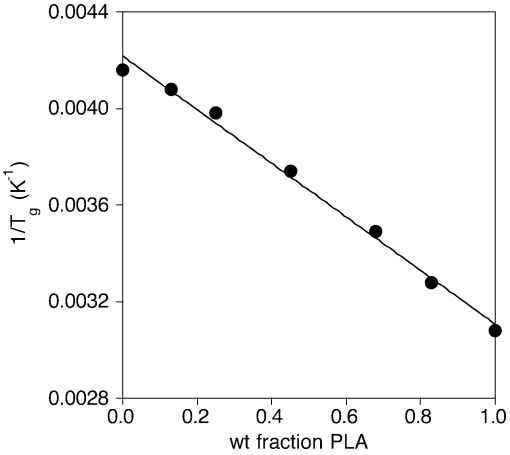

Figure 7. Plot of $1/T_g$ versus PLA weight fraction for blends of *S,S*-PMOD with atactic PLA.

Table 3. Glass Transition Temperatures of *S,S*-PMOD/PLA Blends As Measured by DSC

PLA wt %	T_g (°C)	PLA wt %	T_g (°C)
0	−33.0	0.68	−12.7
0.13	−28.4	0.83	31.0
0.25	−22.0	1	51.0
0.45	−6.3		

Blends of *S,S*-PMOD ($M_n = 18$ kg mol^{-1}, PDI = 1.7) and atactic PLA ($M_n = 66$ kg mol^{-1}, PDI = 1.8) were prepared by mixing solutions of the polymers in various ratios in $CHCl_3$ and then precipitating the mixture by addition of excess hexane. The exact weight percentages of the polymer components were then determined by ^{1}H NMR spectroscopy. DSC experiments showed that each blend exhibits a single glass transition temperature, consistent with the complete miscibility of the two polymers over the entire composition range. Furthermore, the glass transition temperatures of the blend are consistent with the Fox equation for homogeneous binary systems (Figure 7, Table 3)

$$\frac{1}{T_g} = \frac{W_1}{T_1} + \frac{W_2}{T_2} \qquad (3)$$

where W_i is the weight percentage of component i, T_i is the glass transition temperature of component i, and T_g is the glass transition temperature of the blend.[40] In addition, the width of the DSC transition zone for each blend varies, with each being wider than that of either of the constituents (Figure S6). Taken together, the thermal behavior we have measured for the blends supports the potential feasibility of using *S,S*-PMOD as a plasticizer for PLA.

Conclusion

We have prepared a new isotactic polymer (*S,S*-PMOD) comprising perfectly alternating lactic acid and oxetane subunits from an enantiomerically pure 14-membered cyclic diester (*S,S*-**3**), which is derived from a biorenewable resource (ethyl (*S*)-lactate). The ring-opening polymerization of *S,S*-**3** mediated by a highly active zinc alkoxide catalyst occurs at a rate comparable to that of (D,L)-lactide under the same conditions. The polymerization ensues despite the absence of ring strain in *S,S*-**3** (indicated by experimental thermodynamic measurements and theoretical calculations), with a gain of entropy ($\Delta S_p° = +16 \pm 2$ J mol^{-1} K^{-1}) being the

reaction driving force. The new polymer *S,S*-PMOD displays a glass transition temperature of about −30 °C, regardless of the molecular weights studied (5−72 kg mol^{-1}). Importantly, the potential utility of *S,S*-PMOD as a plasticizer for PLA is suggested by its miscibility with atactic PLA in all proportions and its predictable control of the glass transition temperature of the blends.

Experimental Section

General Considerations. All air- or moisture-sensitive compounds were handled under a nitrogen atmosphere, either using standard Schlenk-line techniques or in a glovebox. Toluene, dichloromethane, and pentane used for polymerizations were purified by passing through activated alumina-based columns (Glass Contour, Laguna Beach, CA) and all the other solvents were used as received from a commercial source without further purification. D,L-Lactide was purified by recrystallization from toluene, followed by repeated (2× or 3×) vacuum sublimation. Ethyl (*S*)-lactate (97%), ethyl (*S*/*R*)-lactate, allyl bromide, silver(I) oxide, BH_3·THF (1 M), and *p*-toluenesulfonic acid monohydrate were used as received from Aldrich without further purification. The zinc catalyst was synthesized as previously reported.[25]

NMR spectra were collected on a Varian INOVA-300 or Varian INOVA-500 spectrometer. Chemical shifts were reported in the units of ppm and referenced to the protio impurities in the deuterated solvents for ^{1}H and corresponding ^{13}C resonances. Elemental analyses were determined by Atlantic Microlab, Inc., Norcross, GA. Molecular weights (M_n and M_w) and polydispersity indices (M_w/M_n) were determined by size exclusion chromatography (SEC) using polystyrene standards. Samples were analyzed at 40 °C using a Hewlett-Packard high-pressure liquid chromatography equipped with three Jordi poly(divinylbenzene) columns of 10^4, 10^3, and 500 Å pore sizes and a HP1047A differential refractometer. Differential scanning calorimetry (DSC) was performed on a Perkin-Elmer Pyris I. An indium standard was used for calibration, and nitrogen was used as the purge gas. Samples with a weight range of 4.0−10.0 mg were loaded into aluminum pans, the masses were recorded, and the pans were sealed prior to measurement. Progress of selected polymerizations was monitored using a Mettler Toledo ReactIR 4000 equipped with a diamond probe. Matrix-assisted laser desorption ionization mass spectrometry (MALDI-MS) was performed on a Bruker Reflex III MALDI-TOF mass spectrometer. Samples were deposited in a dithranol/sodium trifluoroacetate matrix. Internal calibration of the instrument was performed using PEO standards. High-resolution mass spectrometry using chemical ionization (HRMS-CI) was performed on a Finnigan MAT 95 (4% NH_3 in CH_4). FT-IR spectra were collected on a Nicolet Magna 550 FT-IR spectrometer. Optical rotation measurements were performed using a JASCO DIP-370 system. GC/MS experiments were performed on a Hewlet-Packard HP G1800A GCD system. Thin-layer chromatography (TLC) was performed on prepared silica gel TLC plates (0.2 mm silica gel 50 F-254, plastic plates). Column chromatography was performed using silica gel 60 (70−230 mesh) with the optimal solvent system determined by TLC.

Ethyl [2-(*S*)-Allyoxy]propanoate (1). Ag_2O (69.6 g, 0.3 mol) was added in portions to a solution of ethyl (*S*)-lactate (35.4 g, 0.3 mol) and allyl bromide (54.5 g, 0.45 mol) in anhydrous diethyl ether (300 mL) under a flow of nitrogen at room temperature with stirring. The mixture was heated to reflux for ∼8 h after the complete addition of Ag_2O. The mixture was then allowed to cool to room temperature and was filtered through Celite. Evaporation of solvent from the filtrate afforded a clear liquid, which was purified by column chromatography to give the desired product (42 g, 89%). R_f = 0.57 (hexane:ethyl acetate = 1:1); $[\alpha]^{25}_D = -67.2$ (*c*, 1.425 g/100 mL, $CHCl_3$); ^{1}H NMR ($CDCl_3$) δ 1.29 (t, J = 7.2 Hz, 3H), 1.40 (d, J = 6.6 Hz, 3H), 3.89−3.95 (m, 1H), 4.00 (q, J = 6.6 Hz, 1H), 4.10−4.15 (m, 1H), 4.20 (q, J = 7.2 Hz, 2H), 5.16−5.32 (m, 2H), 5.31−5.95 (m, 1H) ppm; ^{13}C{^{1}H} NMR ($CDCl_3$) δ 173.6, 134.4, 118.0, 74.2, 71.4, 61.0, 19.0, 14.4 ppm; FTIR (neat, cm^{-1}) 3082, 2985, 2939, 2875, 1749, 1141; HRMS-CI (*m*/*z*) [M + H]$^+$ calcd for $C_8H_{15}O_3$, 159.1385; found 159.1022; [M + NH_4]$^+$ calcd for $C_8H_{18}NO_3$, 176.1650; found 176.1293.

Ethyl [2-(*S*)-Hydroxypropoxy]propanoate (2). BH_3·THF (46 mL, 0.046 mol) was added slowly to neat **1** (19 g, 0.12 mol) under nitrogen at 0 °C. The solution was stirred for 0.5 h at room temperature. Distilled water (3 mL) was then added, followed by an aqueous NaOH solution (3 M, 15.6 mL, 0.046 mol). The reaction mixture was cooled to 0 °C in an ice−water bath and an aqueous H_2O_2 solution (30%, 15.6 mL) was added slowly, keeping the reaction temperature below 25 °C. The mixture was stirred for an additional 1.5 h at room temperature after addition of H_2O_2 was complete. The reaction mixture was then filtered through Celite, anhydrous diethyl ether (40 mL) was added to the filtrate, and the organic layer was separated and washed first with distilled water until pH = 6 and then with a brine solution. The organic layer was separated and dried over anhydrous $MgSO_4$. Filtration and evaporation afforded the product as a clear liquid (14 g, 66%). $[\alpha]^{25}_D = -51.2$ (*c*, 1.43 g/100 mL, $CHCl_3$); ^{1}H NMR ($CDCl_3$) δ 1.28 (t, J = 7.2 Hz, 3H), 1.40 (d, J = 6.6 Hz, 3H), 1.76−1.86 (m, 2H), 2.82 (br s, 1H), 3.64−3.66 (m, 2H), 3.72−3.85 (m, 2H), 3.96 (q, J = 6.6 Hz, 1H), 4.17−4.25 (m, J = 7.2, 2H) ppm; ^{13}C-{^{1}H} NMR ($CDCl_3$) δ 174.0, 75.0, 68.3, 61.3, 60.8, 32.2, 18.9, 14.4 ppm; FTIR (neat, cm^{-1}) 3439, 2984, 2940, 2878, 1734, 1148; HRMS-CI (*m*/*z*) [M + H]$^+$ calcd for $C_8H_{17}O_3$, 177.1127; found 177.1126; [M + NH_4]$^+$ calcd for $C_8H_{20}NO_3$,194.1392; found 194.1390.

6,13-Dimethyl-1,4,8,11-tetraoxacyclotetradecane-2,9-dione (*S,S*-3). *p*-Toluenesulfonic acid monohydrate (0.81 g, 4.2 mmol) was added to a solution of **2** (5 g, 28 mmol) in toluene (330 mL). The solution was heated to reflux for 8 h under a flow of nitrogen. The solution was allowed to cool to room temperature, filtered through Celite, and washed first with distilled water until pH = 6 and then with a brine solution. The organic layer was separated and dried over anhydrous $MgSO_4$. Filtration and evaporation afforded a pale yellow liquid, which was purified by column chromatography to give the desired product, which was recrystallized from hexane to yield a white solid (0.5 g, 14%). R_f = 0.3 (hexane:ethyl acetate = 4:1); mp 78−79 °C; $[\alpha]^{25}_D = -198.9$ (*c*, 1.10 g/100 mL, $CHCl_3$); ^{1}H NMR ($CDCl_3$) δ 1.41 (d, J = 6.6 Hz, 6H), 1.88−2.05 (m, 4H), 3.54−3.58 (m, 2H), 3.67−3.74 (m, 2H), 3.97−4.03 (q, J = 6.6, 2H), 4.25−4.42 (m, 4H) ppm; ^{1}H NMR (C_6D_6) δ 1.33 (d, J = 6.6 Hz, 6H), 1.62 (m, 4H), 3.11 (m, 2H), 3.51 (m, 2H), 3.76 (q, J = 6.8, 2H), 4.20 (m, 4H) ppm; ^{13}C{^{1}H} NMR ($CDCl_3$) δ 173.6, 75.5, 65.5, 61.2, 29.0, 18.6 ppm; ^{13}C NMR (C_6D_6) δ 173.2, 75.8, 65.4, 61.1, 29.3, 18.8 ppm; FTIR (neat, cm-^{1}) 2990, 2971, 2959, 2924, 2896, 2873, 1736, 1202, 1141; HRMS-CI (*m*/*z*) [M + H]$^+$ calcd for $C_{12}H_{21}O_6$, 261.1338; found 261.1325; [M + NH_4]$^+$ calcd for $C_{12}H_{24}NO_6$, 278.1604; found 278.1601. Anal. Calcd ($C_{12}H_{20}O_6$) for C, 55.37; H, 7.74; found C, 55.33; H, 7.72.

A 1:1 mixture of racemic and meso **3** was prepared in the same manner from a racemic precursor [ethyl (*S*/*R*)-lactate]. The meso form of **3** was less soluble in hexane as compared with the racemic form, so by washing the mixture with warm hexane a sample enriched with 90% meso DMOD was obtained. $[\alpha]^{25}_D = 1.3$ (*c*, 3.87 g/100 mL, $CHCl_3$); ^{1}H NMR (C_6D_6) δ 1.29 (d, J = 6.5 Hz, 6H), 1.46 (m, 2H), 1.63 (m, 2H), 2.99 (m, 2H), 3.59 (m, 2H), 3.85 (q, J = 6.5, 2H), 3.98 (dt, J = 10.8, J = 4.3 Hz, 2H), 4.27 (td, J = 11.6, J = 3.0 Hz, 2H) ppm; ^{13}C-{^{1}H} NMR (C_6D_6) δ 173.1, 77.2, 65.4, 60.7, 29.2, 18.7 ppm.

Polymerizations. Polymerization reactions were performed at room temperature in the glovebox. The glassware used was oven-dried, treated with a solution of Me_2SiCl_2 (1.0 M in CH_2Cl_2), and oven-dried at 200 °C for a minimum of 3 h before use. For the purpose of comparison of data among different samples, the initial monomer concentration was kept the same, unless otherwise stated. A stock solution of zinc alkoxide catalyst was prepared such that $[Zn]_0$ = 0.107 M in toluene and was stored under nitrogen at −30 °C. The amount of catalyst used varied depending on the desired molecular

weight of the resulting polymer. A representative procedure is as follows. In the glovebox, a vial was charged with *S,S*-**3** (120 mg, 0.46 mmol) and toluene (254 μL). A volume of the catalyst stock solution (46 μL) was injected in the monomer solution with stirring. The reaction mixture was stirred at room temperature for 20 min. The reaction was then quenched by exposure to the air outside the glovebox. The forming polymer (*S,S*-PMOD) was precipitated by addition of an excess of pentane. The polymer (81 mg, 75%) was separated by decanting, washed with pentane a few times, and dried in vacuo at room temperature. ^{1}H NMR ($CDCl_3$) δ 1.38 (d, J = 6.6 Hz, 6H), 1.94 (m, 4H), 3.38−3.45 (m, 2H), 3.60−3.64 (m, 2H), 3.89−3.96 (m, 2H), 4.19−4.30 (m, 4H) ppm; ^{1}H NMR (C_6D_6) δ 1.35 (d, J = 6.6 Hz, 6H), 1.80 (m, 4H), 3.22 (m, 2H), 3.62 (m, 2H), 3.81 (m, 2H), 4.25 (m, 4H) ppm; ^{13}C{^{1}H} NMR ($CDCl_3$) δ 173.4, 75.2, 66.7, 62.2, 29.3, 19.0 ppm;^{13}C{^{1}H} NMR (C_6D_6) δ 173.1, 75.6, 66.8, 62.3, 29.9, 19.2 ppm.

Atactic PMOD was prepared in the same manner from a 1:1 mixture of racemic and meso **3**. ^{1}H NMR (C_6D_6) δ 1.35 (d, J = 6.6 Hz, 6H), 1.80 (m, 4H), 3.22 (m, 2H), 3.62 (m, 2H), 3.81 (m, 2H), 4.25 (m, 4H) ppm; ^{13}C{^{1}H} NMR (C_6D_6) δ 173.1, 75.66, 75.63, 66.81, 66.78 62.41, 62.35, 29.95, 29.93, 19.21 ppm.

Preparation of Polymer Blends. A sample of *S,S*-PMOD was dried in vacuo at 40 °C overnight (M_n = 18 kg·mol^{-1}, PDI = 1.7). A sample of atactic PLA was synthesized by addition of a solution of zinc alkoxide catalyst (5 mg, 11.6 μmol) in CH_2Cl_2 (0.47 mL) into a solution of D,L-lactide (500 mg, 3.47 mmol) in CH_2Cl_2 (3 mL). The reaction mixture was stirred for 20 min at room temperature and then poured into cold hexane. The product polymer precipitated as a white solid and was dried in vacuo at 80 °C overnight (445 mg, 89%, M_n = 66 kg·mol^{-1}, PDI = 1.8). Separate stock solutions of atactic PLA (0.124 M) and *S,S*-PMOD (0.118 M) in CH_2Cl_2 were used to prepare mixed samples with approximately desired proportions. The solvent was then evaporated in vacuo and the residue dried at 80 °C overnight to yield the polymer blends, the composition of which was quantitated by ^{1}H NMR spectroscopy.

DSC Experiments. A small amount of the polymer or polymer blend was loaded onto an aluminum pan. In the DSC experiment, the sample was heated rapidly from 50 to 150 °C at a rate of 40 °C min^{-1}, whereupon the temperature was held for 5 min to remove all thermal history. The sample was then cooled to −100 °C at a rate of 40 °C min^{-1}, where the temperature was held for another 5 min before heating to 180 °C at a rate of 10 °C min^{-1}. The glass transition temperature (T_g) was determined from the second heating scan by a mathematical averaging method. Straight lines were fit tangent to the heat flow curve before and after the transition. From the average of the slopes and intercepts of these two lines, a third line was obtained, and the T_g was taken as the temperature at which the heat flow curve intersected this third line.

Kinetics Experiments. The progress of a polymerization reaction was monitored in situ by a ReactIR 4000 spectrometer. The reaction vessel containing a solution of monomer and catalyst and the ReactIR probe was preassembled in the glovebox before being quickly attached to the IR spectrometer outside the glovebox. Because of the similarity between the FTIR spectra of *S,S*-**3** and *S,S*-PMOD, the decay of peaks due to *S,S*-**3** was extracted through deconvolution of peaks between 1670 and 1800 cm^{-1} using the built-in program "Concert Opus". An exponential fit of the decay curve using $A_t = (A_0 - A_\infty)e^{-kt} + A_\infty$ gave the observed rate constant k_{obs}. After the reaction reached equilibrium (no discernible FTIR spectral changes), an aliquot of the reaction mixture was removed, and the conversion and equilibrium monomer concentration ($[\mathbf{3}]_{eq}$) were determined by ^{1}H NMR spectroscopy.

Polymerization Thermodynamics Experiments. In the glovebox, an aliquot of a stock solution of the zinc alkoxide catalyst in toluene (46 μL, 0.107 M) was added to a solution of *S,S*-**3** (120 mg, 0.461 mmol) in toluene (254 μL) in a vial with a stir bar. The vial was sealed, removed from the glovebox, and submerged in a preset temperature-controlled bath (between 0 and 100 °C) for 1 h with stirring. The reaction was quenched by exposing the reaction mixture to the air for 5 min, while the vial was still sitting in the temperature-controlled bath. Removal of an aliquot and analysis by ^{1}H NMR spectroscopy enabled the equilibrium monomer concentration to be determined (0.154 M under these conditions). Alternatively, the equilibrium monomer concentration at different temperatures was obtained from a variable-temperature ^{1}H NMR experiment. A representative procedure is as follows. In the glovebox, deuterated toluene (0.7 mL) was added to a Young's cap NMR tube charged with *S,S*-**3** (109 mg, 0.420 mmol) and the zinc alkoxide catalyst (4.8 mg, 0.0112 mmol). The VT ^{1}H NMR experiment was performed between 20 and 60 °C and a conversion of 68−70% was observed in the temperature range studied. Thus, the equilibrium concentration of *S,S*-**3** was determined to be 0.180−0.188 M under these conditions. To ensure that the catalyst was still active after the VT NMR experiment, an additional amount of *S,S*-**3** (55 mg, 0.211 mmol) was added into the NMR tube inside the glovebox. ^{1}H NMR spectroscopic analysis showed that the additional *S,S*-**3** was polymerized and a conversion of ∼80% was observed.

Computational Methods. All structures were fully optimized at the Hartree−Fock level of theory[41] using the MIDI! basis set.[42] To identify the minimum-energy structure, sets of conformers for all molecules were initially generated by two methods. First, structures were generated by extensive manual rotations about single bonds followed by minimization using the MM2 molecular mechanics force field.[43] In addition, separate sets of MM2 minima were identified from Monte Carlo stochastic search strategies. The 10−20 lowest energy distinct conformers from these two approaches were then subjected to HF/MIDI! Optimization, and the global minima were selected from the HF results. Continuum solvation free energies were computed for all species at the SM5.42R/HF/MIDI! level[44] using both ethyl acetate and toluene as solvents. Single-point electronic structure calculations were also carried out at the B3LYP density functional level[45] using the 6-31G-(d) basis set.[46] Conclusions derived from the solvation and B3LYP calculations did not differ qualitatively from those determined at the more computationally efficient HF/MIDI! level and are therefore not further discussed. Electronic structure calculations were carried out using the Gaussian program suite.[47] MM2 calculations with and without Monte Carlo sampling were carried out using Chem-3D[48] and MacroModel,[49] respectively.

Acknowledgment. We thank the NSF (CHE-0236662 and CHE-0203346) and the David and Lucile Packard Foundation for financial support of this research.

Supporting Information Available: ^{1}H NMR spectra for **3** and PMOD, MALDI-MS spectrum of high molecular weight PMOD in the low *m/z* region, a representative kinetic trace for the polymerization of *S,S*-**3**, a plot of $\Delta H_p°$ versus ΔE values, DSC traces, FTIR spectra for *S,S*-**3** and *S,S*-PMOD, and X-ray crystallographic data. This material is available free of charge via the Internet at http://pubs.acs.org.

References and Notes

(1) Drumright, R. E.; Gruber, P. R.; Henton, D. E. *Adv. Mater.* **2000**, *12*, 1841.
(2) Leeson, E. J. *Rubber World* **1967**, *157*, 62.
(3) Maura, G.; Rinaldi, G. *Macromol. Symp.* **2001**, *176*, 39.
(4) Kramer, S. *Plastverarbeiter* **1988**, *39*, 23.
(5) Wilson, A. S., *Plasticisers: Principles and Practice*; The Institute of Materials: London, 1995.
(6) Ohkoshi, I.; Abe, H.; Doi, Y. *Polymer* **2000**, *41*, 5985.
(7) Maglio, G.; Migliozzi, A.; Palumbo, R.; Immirzi, B.; Volpe, M. G. *Macromol. Rapid Commun.* **1999**, *20*, 236.
(8) Maglio, G.; Migliozzi, A.; Palumbo, R. *Polymer* **2003**, *44*, 369.
(9) Lostocco, M. R.; Borzacchiello, A.; Huang, S. J. *Macromol. Symp.* **1998**, *130*, 151.
(10) Martin, O.; Avèrous, L. *Polymer* **2001**, *42*, 6209.
(11) Sinclair, R. G. *J. Macromol. Sci., Pure Appl. Chem.* **1996**, *A33*, 585.

(12) Nijenhuis, A. J.; Colstee, E.; Grijpma, D. W.; Pennings, A. J. *Polymer* **1996**, *37*, 5849.
(13) Sheth, M.; Kumar, R. A.; Davè, V.; Gross, R. A.; McCarthy, S. P. *J. Appl. Polym. Sci.* **1997**, *66*, 1495.
(14) Yang, J.-M.; Chen, H.-L.; You, J.-W.; Hwang, J. C. *Polym. J. (Tokyo)* **1997**, *29*, 657.
(15) Hu, Y.; Rogunova, M.; Topolkaraev, V.; Hiltner, A.; Baer, E. *Polymer* **2003**, *44*, 5701.
(16) Gajria, A. M.; Davè, V.; Gross, R. A.; McCarthy, S. P. *Polymer* **1996**, *37*, 437.
(17) Park, J. W.; Im, S. S. *J. Appl. Polym. Sci.* **2002**, *86*, 647.
(18) Park, J. W.; S., I. S. *J. Polym. Sci. Part B: Polym. Phys.* **2002**, *40*, 1931.
(19) Lostocco, M. R.; Huang, S. J. *J. Macromol. Sci., Pure Appl. Chem.* **1997**, *A34*, 2165.
(20) Ljungberg, N.; Wesslèn, B. *Polymer* **2003**, *44*, 7679.
(21) Bechtold, K.; Hillmyer, M. A.; Tolman, W. B. *Macromolecules* **2001**, *34*, 8641.
(22) Jacobsen, S.; Fritz, H. G. *Polym. Eng. Sci.* **1999**, *39*, 1303.
(23) Brandrup, J.; Immergut, E. H.; Grulke, E. A. *Polymer Handbook*; John Wiley-Interscience: New York, 1999.
(24) Broggini, G.; Molteni, G.; Pilati, T. *Tetrahedron: Asymmetry* **2000**, *11*, 1975.
(25) Williams, C. K.; Breyfogle, L. E.; Choi, S. K.; Nam, W.; Young, V. G., Jr.; Hillmyer, M. A.; Tolman, W. B. *J. Am. Chem. Soc.* **2003**, *125*, 11350.
(26) The direction chosen for consideration in Figure 4 is arbitrary; the methine carbon chemical shift could equally as likely be affected by stereogenic centers positioned in the opposite direction along the polymer chain than shown.
(27) Duda, A.; Penczek, S. *Biopolymers*; Wiley-VCH: Weinheim, 2001; Vol. 3b, pp 371−429.
(28) Libiszowski, J.; Kowalski, A.; Szymanski, R.; Duda, A.; Raquez, J.-M.; Degée, P.; Dubois, P. *Macromolecules* **2004**, *37*, 52.
(29) Fey, T.; Keul, H.; Hocker, H. *Macromolecules* **2003**, *36*, 3882.
(30) Dainton, F. S.; Ivin, K. J. *Quart. Revs. (London)* **1958**, *12*, 61.
(31) Hodge, P.; Kamau, S. D. *Angew. Chem., Int. Ed.* **2003**, *42*, 2412.
(32) Kamau, S. D.; Hodge, P.; Helliwell, M. *Polym. Adv. Technol.* **2003**, *14*, 492.
(33) Hodge, P. *React. Funct. Polym.* **2001**, *48*, 15.
(34) Hall, A. J.; Hodge, P. *React. Funct. Polym.* **1999**, *41*, 133.
(35) Evstropov, A. A.; Lebedev, B. V.; Kiparisova, E. G. *Vysokomol. Soedin.* **1983**, *A25*, 1679.
(36) For other model ring-strain definitions, see: March, J., *Advanced Organic Chemistry*, 4th ed.; John Wiley & Sons: New York, 1992; pp 150−157.
(37) Duda, A.; Penczek, S. *Macromolecules* **1990**, *23*, 1636.
(38) Nishida, H.; Yamashita, M.; Endo, T.; Tokiwa, Y. *Macromolecules* **2000**, *33*, 6982.
(39) Save, M.; Schappacher, M.; Soum, A. *Macromol. Chem. Phys.* **2002**, *203*, 889.
(40) Fox, T. G. *Bull. Am. Phys. Soc.* **1956**, *1*, 123.
(41) Cramer, C. J. *Essentials of Computational Chemistry: Theories and Models*; Wiley: Chichester, 2002.
(42) Easton, R. E.; Giesen, D. J.; Welch, A.; Cramer, C. J.; Truhlar, D. G. *Theor. Chim. Acta* **1996**, *93*, 281.
(43) Burkert, U.; Allinger, N. L. *Molecular Mechanics*; ACS Monograph 177; American Chemical Society: Washington, DC, 1982.
(44) Li, J.; Hawkins, G. D.; Cramer, C. J.; Truhlar, D. G. *Chem. Phys. Lett.* **1998,** *288*, 293.
(45) (a) Becke, A. D. *Phys. Rev. A* **1988**, *38*, 3098. (b) Becke, A. D. *J. Chem. Phys.* **1993**, *98*, 5648. (c) Lee, C.; Yang, W.; Parr, R. G. *Phys. Rev. B* **1988**, *37*, 785. (d) Stephens, P. J.; Devlin, F. J.; Chabalowski, C. F.; Frisch, M. J. *J. Phys. Chem.* **1994**, *98*, 11623.
(46) Hehre, W. J.; Radom, L.; Schleyer, P. v. R.; Pople, J. A. *Ab Initio Molecular Orbital Theory*; Wiley: New York, 1986; pp 79−82.
(47) Frisch, M. J.; Trucks, G. W.; Schlegel, H. B.; Scuseria, G. E.; Robb, M. A.; Cheeseman, J. R.; Montgomery, J. A.; Vreven, T.; Kudin, K. N.; Burant, J. C.; Millam, J. M.; Iyengar, S. S.; Tomasi, J.; Barone, V.; Mennucci, B.; Cossi, M.; Scalmani, G.; Rega, N.; Petersson, G. A.; Nakatsuji, H.; Hada, M.; Ehara, M.; Toyota, K.; Fukuda, R.; Hasegawa, J.; Ishida, M.; Nakajima, T.; Honda, Y.; Kitao, O.; Nakai, H.; Klene, M.; Li, X.; Knox, J. E.; Hratchian, H. P.; Cross, J. B.; Adamo, C.; Jaramillo, J.; Gomperts, R.; Stratmann, R. E.; Yazyev, O.; Austin, A. J.; Cammi, R.; Pomelli, C.; Ochterski, J. W.; Ayala, P. Y.; Morokuma, K.; Voth, G. A.; Salvador, P.; Dannenberg, J. J.; Zakrzewski, V. G.; Dapprich, S.; Daniels, A. D.; Strain, M. C.; Farkas, O.; Malick, D. K.; Rabuck, A. D.; Raghavachari, K.; Foresman, J. B.; Ortiz, J. V.; Cui, Q.; Baboul, A. G.; Clifford, S.; Cioslowski, J.; Stefanov, B. B.; Liu, G.; Liashenko, A.; Piskorz, P.; Komaromi, I.; Martin, R. L.; Fox, D. J.; Keith, T.; Al-Laham, M. A.; Peng, C. Y.; Nanayakkara, A.; Challacombe, M.; Gill, P. M. W.; Johnson, B.; Chen, W.; Wong, M. W.; Gonzalez, C.; Pople, J. A. *Gaussian 03 (Revision B.01)*; Gaussian, Inc.: Pittsburgh, PA, 2003.
(48) *ChemBats3D*, version 5.0, CambridgeSoft Inc.
(49) *MacroModel*, version 6.0, Schrödinger LLC.

MA049571S